Surface Charging Analysis of High-Inclination, High-Altitude Spacecraft: Identification and Physics of the Plasma Source Region

Harlan E. Spence, J. Bernard Blake, and Joseph F. Fennell
Space and Environment Technology Center, The Aerospace Corporation,
Los Angeles, CA 90009

Abstract

We have identified surface charging as the probable cause of anomalies experienced by several high-inclination, high-altitude spacecraft. These spacecraft have no monitors of the local space particle environment. Thus a direct association of anomaly occurrence with surface discharge is not possible. Rather, we use empirical magnetic-field models to map from a satellite's position, at the time of an anomaly, to the Earth's magnetospheric equatorial plane. We appeal to the well-established occurrence distribution of spacecraft charging in the near-geostationary orbit equatorial plane as a function of magnetic local time, radial distance, and geomagnetic activity to interpret the anomaly events. On the basis of the similarity between known surface charging distributions and the anomaly distributions, we conclude that anomaly associated surface charging likely occurred owing to transient hot plasma and medium-energy electrons associated with magnetospheric substorms. We believe that this technique will aid satellite operators in the assessment of anomalies experienced by high-inclination spacecraft.

I. Introduction

Hot plasmas and medium-energy electrons (< 50 keV) are a well-known source of differential charging on space vehicles in the geostationary orbit [1,2]. The P78-2 (SCATHA) satellite, for example, provided direct *in situ* evidence of surface discharges in association with the injection of hot plasma and energetic electrons into the vicinity of near-geostationary orbit [3]. Surface discharges may produce unexpected current pulses on a satellite's electrical system and, thus, adversely affect its control circuits and lead to operational anomalies. The detailed physics of spacecraft charging and it's related deleterious effects are beyond the scope of this paper; Garrett [4] provides an extensive review of these topics.

The space plasma physics community has studied extensively the morphology and dynamics of those charged particles in the vicinity of the near-geostationary magnetospheric equatorial plane that are responsible for spacecraft charging. In this paper, we focus on and appeal to this knowledge in assessing anomalies of high-inclination (i.e., off-equatorial) satellites. As well, we outline the technique of using empirical magnetospheric magnetic-field models to provide the linkage between an arbitrary spacecraft location and its particle source region at the equatorial plane. This study demonstrates the utility of these models as an anomaly diagnosis tool.

II. The Geostationary Environment, Substorms, and Surface Charging

Transient and localized hot plasmas are injected into the inner magnetosphere (L ~ 6.6), near local midnight, at the onset of geomagnetic substorms [5]. L is approximately the number of Earth radii (R_E) to a point in space (at the magnetic equator) from the center of the Earth. The energized plasma drifts in the Earth's quasi-dipolar magnetic field according to the combined effects of the corotation and crosstail convection electric fields, magnetic field-gradient forces, and magnetic field-curvature forces. Following their energization and injection into the near-geostationary environment, the bulk plasma and medium-energy electrons drift eastward (i.e., toward dawn from midnight) along, to first order, a fixed L-shell. Figure 1 illustrates these effects schematically.

Therefore, following a substorm onset, an abrupt energization of the hot plasma and medium-energy electrons characterize the post-midnight plasma environment at near-geostationary orbit. The temporal variations associated with substorm onsets appear as spatial gradients of the particle population in the spacecraft's rest frame. These gradients may establish the differential charging on spacecraft surfaces that leads to arcing.

The injected hot plasma and medium-energy charged particles generally have velocity components both perpendicular and parallel to the local magnetic-field direction. These populations are thus distributed along tubes of magnetic flux and are trapped. Consequently, the effects of the plasma injection

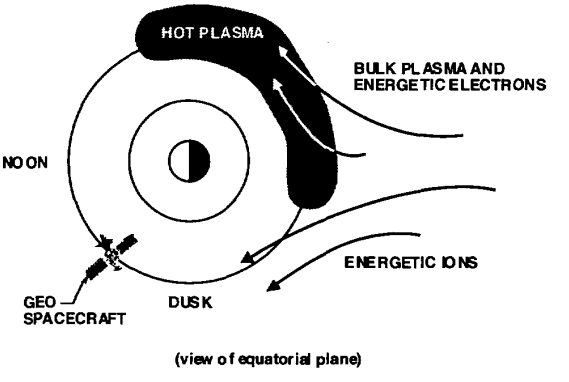

Fig. 1. Schematic, in the magnetospheric equatorial plane, of hot plasma and energetic particle injection into the near-geostationary region at substorm onset. The eastward-drifting, hot plasma and medium-energy electrons can lead to surface discharge events in the dawn sector.

0018-9499/93$03.00 © 1993 IEEE

are not only evident to geostationary satellites near the magnetic equatorial plane, but also should be experienced by high-inclination satellites that connect magnetically to the particle regions near the equatorial plane.

In this study, we establish that the magnetic linkage and phenomenology of the majority of the anomalies observed by several high-inclination spacecraft are consistent with the known physics of surface charging at geostationary locations. In addition, we feel that this study demonstrates the utility of magnetic-field models for aiding the diagnosis of off-equatorial anomalies. We propose that such a technique may be extremely useful to satellite operators and contractors who wish to differentiate spacecraft anomaly sources on those satellites operating in an otherwise poorly monitored region of space.

III. Observations

We analyzed a data base of approximately 100 anomalies, experienced by several high-inclination, high-altitude satellites, in order to establish their probable cause. These anomalies occurred over the span of nearly a decade. The data base contained the spacecraft position in geographic coordinates, the date and time, and the Kp index for each anomaly occurrence. It is important to note that the anomalies experienced by these satellites were substantially similar in nature, and that all spacecraft were identically designed.

A. Kp Dependence

The Kp index provides an indirect, quantitative measure of the geomagnetic activity in the magnetosphere and is related approximately to the number and size of geomagnetic substorms and storms during a given three-hour interval. Mayaud presents a thorough discussion of the derivation and significance of the Kp value [6]. In short, the Kp index is derived from magnetic fluctuations measured globally at the Earth's surface and its value ranges from 0 to 9 on a quasi-logarithmic scale; 0 is indicative of a period of extreme geomagnetic quiescence, whereas 9 occurs only during periods of extreme geomagnetic disturbance.

According to the discussion outlined in the introduction, if surface discharges are the source of the anomalous signals, then we should expect the anomaly occurrence to be strongly dependent on the Kp index value. This positive correlation has previously been demonstrated statistically using the SCATHA surface potential monitor data [3]. We find that this type of relationship is strongly present in the high-inclination spacecraft anomaly data base.

As geomagnetic activity increases (i.e., as the Kp index increases), the likelihood for particle energization and hot plasma injection at geostationary orbit also increases, thereby creating the conditions during which surface-charging anomalies occur. This feature is evident in Figure 2 that plots the high-inclination anomaly occurrence rate as a function of Kp (solid curve). With increasing Kp, the anomaly occurrence rate observed by the high-inclination satellites increases

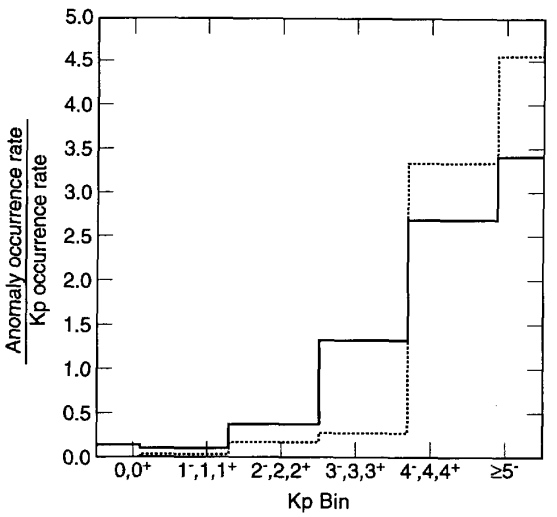

Fig. 2. Anomaly occurrence rate (normalized by the Kp occurrence rate) as a function of Kp (solid curve). The equatorial surface discharge rate determined by SCATHA [3] is shown for comparison (dashed curve).

markedly. (Note that the Kp occurrence rate, which peaks at Kp ~ 2, normalizes the anomaly occurrence rate in order to remove any Kp-occurrence-rate bias.) The anomaly distribution with Kp compares favorably with the known behavior of surface discharges at near-geostationary orbit [3] (dashed curve).

However, Kp-dependence alone is not sufficient to support strongly the supposition that the anomalies uniquely arise from surface electrostatic discharges. Both surface discharge and internal (or alternatively thick dielectric) discharge rates behave similarly with an increasing Kp index [3]. Therefore, we must call upon other anomaly characteristics that can distinguish between a surface and an internal discharge mechanism. In this instance, we look to the occurrence rate as a function of local time and radial distance as an effective distinguisher.

B. Spatial Dependence

We should expect strong spatial dependencies for anomalies related to both surface and bulk discharges. Both types of charging distributions in the near-geostationary, equatorial plane are well established. Extensive statistical surveys of, primarily, the ATS-6 [2] and SCATHA [3, 7, 8] satellites provided occurrence maps of discharge events in the near-magnetic-equatorial plane, near geostationary orbit. Surface discharges occur predominantly on near-geostationary L-shells (~5 to ~12). Their rate is fairly uniform between L = 5 to 8 and drops somewhat at greater distances. On the other hand, internal or bulk discharge rates peak much more clearly at smaller L-shells (< 6 Re) and drop sharply with increasing radial distance.

An even more striking discriminator between the two discharge types is their relative occurrence in magnetic local

time. It has been demonstrated that internal discharges are distributed relatively uniformly in local time with a small but discernible tendency toward dayside local times and a weak peak near 1200 MLT [3]. On the other hand, surface discharges occur nearly exclusively in the dawnside sector, with a fairly strong peak near 0000 MLT and a broad distribution between 0000 and 1000 MLT [3]. Surface discharges are seldom seen in the post-noon, dayside quadrant. Therefore, we construct and investigate these two distributions from the anomaly data base in the following section.

C. Mapping to the Equatorial Plane

In order to assess any similarity between the anomaly occurrence at the high-inclination spacecraft and the well-studied equatorial plane phenomenology, we turned to empirical magnetic-field models. Such models provide the average magnetic-field vector throughout large portions of the magnetosphere for a given date, time, and level of geomagnetic activity. For this analysis, we used the empirical magnetospheric magnetic-field model of Tsyganenko [9]. The Tsyganenko model, which is parameterized by the Kp index, was used to map from the high-inclination spacecraft position at the time of the anomaly, along a magnetic field line, to the field line's magnetic equatorial crossing. (The point at which the magnetic-field magnitude is at a minimum along a field line defines the magnetic equatorial crossing point.)

These mappings established the magnetic, and hence particle, connectivity between a high-inclination, high-altitude spacecraft and the magnetospheric equatorial plane. Figure 3 illustrates strikingly that ≥2/3 of the anomaly occurrences map into the near-geostationary equatorial plasma environment and ≥~90% of those map within the dawn sector between 0000 MLT and 1000 MLT. Furthermore, the occurrence rate with radial distance is approximately uniform over the range of 5 Re to ~10 Re; the rate drops at greater distances.

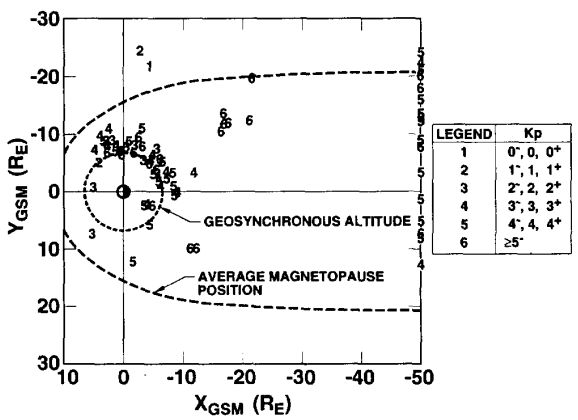

Fig. 3. A view, in the magnetospheric equatorial plane, of the mapped spacecraft locations at the time of the anomaly. The sun is toward the left; the Y_{GSM} axis is the dawn-dusk terminator with dawn toward the top. The average magnetopause position and geosynchronous location are included for reference.

The occurrence rate dependencies displayed in Figures 2 and 3 are qualitatively similar to those demonstrated previously for surface discharges in the near-geostationary region. These similarities are illustrated more clearly in Figures 4 and 5. Figure 4 is a plot of the relative occurrence rate with radial distance in the equatorial plane, between L = 5.2 and 7.8 (i.e., the SCATHA orbital limit). The dashed curve is the relative occurrence rate of surface discharges detected by the SCATHA satellite [3], and the solid curve is the anomaly rate inferred from the high-inclination satellites only over the SCATHA

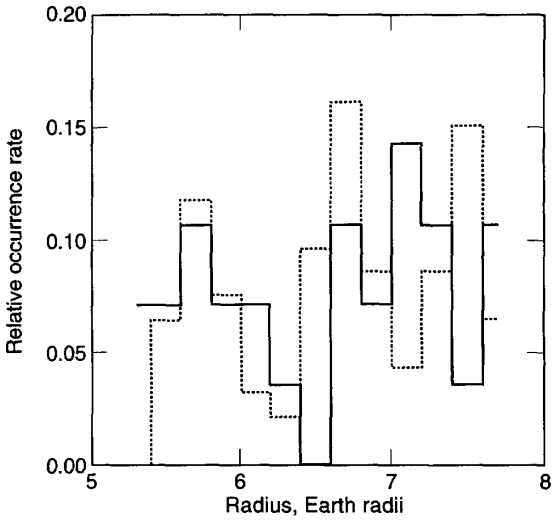

Fig. 4. Anomaly relative occurrence rate as a function of radial distance (solid curve) over the SCATHA range of coverage. The equatorial surface discharge rate determined by SCATHA [3] is shown for comparison (dashed curve).

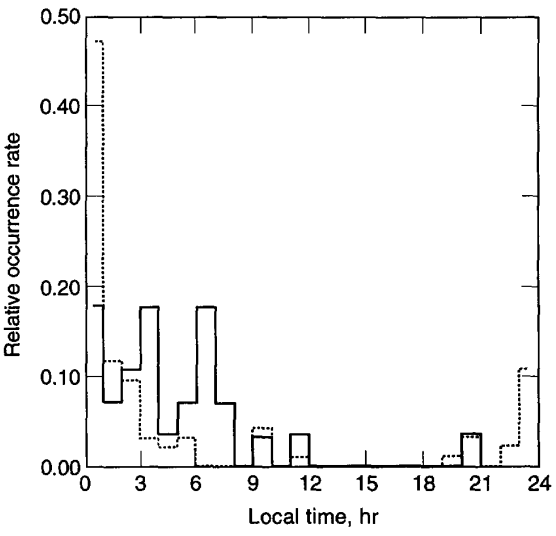

Fig. 5. Anomaly relative occurrence rate as a function of local time (solid curve). The equatorial surface discharge rate determined by SCATHA [3] is shown for comparison (dashed curve); the large peak at midnight is contributed to by eclipse geometries not relevant to the high-inclination sataellites.

range. Both distributions are relatively uniform over these radial distances; there is no evidence for a strong peak at L < 6 characteristic of internal discharges [3]. Figure 5 is a similar plot illustrating the relative occurrence rate as a function of local time (again, only between L =5.2 and 7.8). Both distributions peak in the post-midnight quadrant and drop substantially in the post-noon quadrant. The large surface discharge peak observed by equatorial spacecraft near 00 LT is biased by known eclipse geometries [3]. These midnight eclipse geometries are not relevant for the high-inclination satellites, and this contributes to the large rate differential between the solid and dashed curves near 00 LT. These distributions are fundamentally different from that of internal discharges that peak near noon [3].

IV. Discussion and Conclusions

We established that the majority of anomalies experienced on several high-inclination, high-altitude spacecraft occurred preferentially when the geomagnetic activity index was high and when the vehicle connected magnetically to the dawnside, near-geostationary plasma and particle environment. By appealing to the known dependencies of anomalies observed by near-geostationary satellites, we believe that surface charging is the likely cause of most of these high-inclination anomalies. For the anomalies that possess the characteristics preferred for a surface-charging hypothesis, a probable scenario is as follows. Newly injected electrons and warm plasma differentially charge the surface dielectric material on the spacecraft. At some time, the potential difference between adjoining spacecraft surfaces exceeds a critical value, and arcing occurs. This leads to an anomalous current pulse that couples into the electronics and triggers an operational anomaly. For instance, SCATHA data revealed that resultant voltage spikes can reach magnitudes of many volts, even with large circuit loads (i.e., 50 ohms) present.

The remaining anomalies (i.e., those far from geostationary orbit or in the dusk, dayside vicinity) have physical source mechanisms that are less clear. For instance, as noted earlier, anomalies that occur at near-geostationary locations, but not in the dawn sector, may be attributable to bulk or deep dielectric discharges. SCATHA data show that bulk charging events at geostationary orbit occur when surface charging is absent and during prolonged periods of enhanced energetic electron (> 100 keV) fluxes [3].

In other cases, proper identification may be hindered because the magnetic-field mapping may be in error. Presently available empirical, magnetospheric magnetic-field models may not provide accurate enough mappings to L ≥ 10, particularly during periods of large Kp when a static magnetic-field model is suspect. We have also implicitly assumed that the vehicle connects magnetically with the causative plasma source region when an anomaly occurs. In practice, however, discharges may not occur until after the vehicle has passed through those flux tubes connected to the relevant plasma environment. Such a time delay, even a relatively short one, may cause the mapped plasma source region to be in error and may also contribute to the ~1/3 of all anomalies not described by the above analysis (i.e., those mapping to large distances in the anti-sunward direction).

We believe that this study points to a general spacecraft anomaly diagnosis tool. Mapping, along magnetic flux tubes calculable from an empirical magnetic field model, to the magnetospheric equatorial plane allows for analysis in a region that is well monitored, modeled, and understood. As field models improve and become more user-friendly, association of an anomaly at some general location to a known plasma source region may greatly enhance a satellite operator's ability to identify and assess its possible physical source mechanisms. We are presently working toward these goals [10, 11].

V. Acknowledgments

This work was supported by the Air Force Material Command's Space and Missile Systems Center (SMC) under contract F04701-88-C-0089.

VI. References

[1] S. E. DeForest, "Spacecraft charging at synchronous orbit," *J. Geophys. Res.*, vol. 77, pp. 651- 659, 1972.

[2] D. L. Reasoner, W. Lennartsson, and C. R. Chappell, "Relationship between ATS-6 spacecraft charging occurrences and warm plasma encounters," *Spacecraft Charging by Magnetospheric Plasmas, (Progress in Astronautics and Aeronautics, 47)*, edited by A. Rosen, pp. 89-102, MIT Press, Cambridge, Mass., 1976.

[3] H. C. Koons and D. J. Gorney, "The relationship between electrostatic discharges on Spacecraft P78-2 and the electron environment," *J. Spacecr. Rockets,* vol. 28, p. 683, 1991.

[4] H. B. Garrett, "The charging of spacecraft surfaces," *Rev. Geophys. Space Phys.*, vol. 19, pp. 577-616, 1981.

[5] S. E. DeForest and C. E. McIlwain, "Plasma clouds in the magnetosphere," *J. Geophys. Res.,* vol. 76, pp. 3587-3611, 1971.

[6] P. N. Mayaud, in *Derivation, Meaning, and Use of Geomagnetic Indices*, American Geophysical Union Monograph 22, Washington, DC, 1980, pp. 42-51.

[7] P. F. Mizera and G. M. Boyd, "The satellite surface potential survey," in *Spacecraft charging conference III (1980)*, AFGL-TR-81-0270, pp. 461-469, 1981.

[8] D. A. McPherson and W. R. Schober, "Spacecraft charging at high altitudes: The SCATHA satellite program," *Spacecraft Charging by Magnetospheric Plasmas, (Progress in Astronautics and Aeronautics, 47)* edited by A. Rosen, pp. 15-30, MIT Press, Cambridge, Mass., 1976.

[9] N. A. Tsyganenko, "Global quantitative models of the geomagnetic tail in the cislunar magnetosphere for different disturbance levels," *Planet. Space Sci.*, vol. 35, p. 1347, 1987.

[10] T. I. Pulkkinen *et al.*, "Modelling of the growth phase of a substorm using the Tsygenenko model and multispacecraft observations: CDAW-9," *Geophys. Res. Lett.*, vol. 18, pp. 1963-1966, 1991.

[11] A. T. Y. Lui, H. E. Spence, and D. P. Stern, "Empirical modeling of the quiet time nightside magnetosphere," *J. Geophys. Res.*, in press, 1993.